Raman spectroscopic studies of carbonates, part I: high-pressure and high-temperature behaviour of calcite, magnesite, dolomite and aragonite, Phys. Chem. Minerals 20, 1-18

ARTICLE *in* PHYSICS AND CHEMISTRY OF MINERALS · APRIL 1993

Impact Factor: 1.54 · DOI: 10.1007/BF00202245

4 AUTHORS, INCLUDING:

Philippe Gillet
École Polytechnique Fédérale de Lausanne
265 PUBLICATIONS **6,346** CITATIONS
SEE PROFILE

Bruno Reynard
CNRS
179 PUBLICATIONS **3,155** CITATIONS
SEE PROFILE

Paul F. McMillan
University College London
404 PUBLICATIONS **11,592** CITATIONS
SEE PROFILE

Phys Chem Minerals (1993) 20:1–18

PHYSICS AND CHEMISTRY OF MINERALS

Raman Spectroscopic Studies of Carbonates Part I: High-Pressure and High-Temperature Behaviour of Calcite, Magnesite, Dolomite and Aragonite

Philippe Gillet*, Claudine Biellmann, Bruno Reynard, and Paul McMillan**

Laboratoire de Minéralogie Physique, Rennes Géosciences (UPR CNRS 4661), Université de Rennes I, Institut de Géologie, F-35042 Rennes Cedex, France

Received July 14, 1992/Revised, accepted January 9, 1993

Abstract. The room-temperature Raman spectra of aragonite, magnesite and dolomite have been recorded up to 30 GPa and 25 GPa, respectively and no phase changes were observed during compression, unlike calcite. The effect of temperature on the room-pressure Raman spectra of calcite, aragonite, magnesite and dolomite is reported up to 800–1100 K. The measured relative pressure and temperature-shifts of the Raman lines are greater for the lattice modes than for the internal modes of the CO_3 groups. These shifts are used to calculate the mode anharmonic parameters of the observed Raman modes; they are negative and their absolute values are smaller (close to 0) for the internal CO_3 modes than for the lattice modes (4–17 10^{-5} K^{-1}). The temperature shifts of the lattice modes in calcite are considerably larger than those for dolomite and magnesite, and a marked non-linear increase in linewidth is observed above 400° C for calcite. This is consistent with an increasing relaxational component to the libration of the CO_3 groups about their threefold axes, premonitory to the rotational order-disorder transition at higher temperature. This behaviour is not observed for the other calcite structured minerals in this study. We examine systematic variations in the lattice mode frequencies and linewidths with composition, to begin to understand these differences in their anharmonic behaviour. Finally, we have used a simple Debye-Waller model to calculate atomic displacements in calcite, magnesite and dolomite with increasing temperature from the vibrational frequency data, to provide a direct comparison with atomic positional data from high-temperature structure refinements.

Introduction

The stability of carbonates at very high pressures (P) and temperatures (T) (i.e., under conditions characteristic of the Earth's mantle) is poorly known. Most of the existing experimental studies have been devoted to their stability and reactivity under crustal metamorphic or shallow mantle conditions, rarely in excess of 3 GPa and 1300 K (e.g. Irving and Wyllie 1975). However, some recent experimental investigations (Katsura and Ito 1990) have pointed out that under (P, T) conditions relevant to the Earth's upper and lower mantle, carbonates may be stable phases and may also react with silicates, providing possible host mineral structures for the carbon in the deep mantle. It is therefore of importance to document the behaviour of carbonates at very high pressures and temperatures in order to address several major problems like the generation of carbonated magmas, or the amount of primitive nebular carbon incorporated during Earth's accretion and still trapped in the mantle.

We have recently undertaken an experimental study on the behaviour of carbonates at the pressure and temperature conditions of the Earth's mantle. One part of this work is devoted to the stability of carbonates and their reactivity with silicates (Biellmann et al. 1992). The other part, developed in this paper, concerns the structural response of different carbonates to pressure and temperature as determined by Raman spectroscopy. These spectroscopic measurements permit detection of phase changes, and also provide information on the pressure and temperature-induced structural modifications. Furthermore the spectroscopic data may also be used to predict the thermodynamic properties of minerals under the extreme (P, T) conditions of the mantle (e.g. Gillet et al. 1991).

Carbonates have been extensively studied by Raman spectroscopy at ambient conditions (e.g. Couture 1947; Krishnamurti 1956, 1957; Porto et al. 1966; Griffith 1969; Rutt and Nicola 1974; White 1974; Frech et al. 1980; Bischoff et al. 1985). Several in-situ spectroscopic studies have also been carried out at high P and T. Fong

* *Present address:* Laboratoire des Sciences de la Terre (CNRS URA 726), Ecole Normale Supérieure de Lyon, 46 allée d'Italie, F-69354 Lyon 07, France

** *Permanent address:* Department of Chemistry, Arizona State University, Tempe, AZ 85287, USA

and Nicol (1971), Gillet et al. (1988) and Liu and Mernagh (1990) have reported the room temperature changes in Raman spectra occurring at the calcite I-calcite II (1.4 GPa) and calcite II-calcite III (1.9 GPa) transitions (Bridgman 1939; Merrill and Bassett 1975; Vo-Than and Lacam 1984). Salje and Viswanathan (1976) have studied the effect of pressure up to 0.3 GPa on the Raman spectra of calcite and aragonite and also the effect of temperature on the same minerals up to 800–1000 K. More recently, Kraft et al. (1991) have obtained Raman as well as IR data at room temperature up to 28 GPa on aragonite, dolomite and at 550 K and 10.4 GPa on dolomite. In this latter study, no phase changes were observed in aragonite and dolomite during pressurization in contrast with the phase changes observed in calcite at 1.4 and 1.8 GPa (Fong and Nicol 1971; Gillet et al. 1988; Liu and Mernagh 1990).

In this paper we report the effect of pressure (at room temperature) up to 25–30 GPa and the effect of temperature up to 800–1100 K (at room pressure) on the Raman spectra of calcite, magnesite, dolomite and aragonite. The present data are useful for intercomparison purposes with previous work. They are also more comprehensive than the previous results because all the Raman active modes of calcite, magnesite and dolomite have been tracked at high pressures and high temperatures. This permits assessment of mode anharmonic parameters for calculation of thermodynamic properties for these carbonate minerals, and also to gain a better understanding of the rotational order-disorder transition in calcite at high temperature (Megaw 1970; Redfern et al. 1989; Dove and Powell 1989). In this work, we have also examined structural systematics to achieve insights into the variation of mode frequencies and anharmonicities with composition in calcite and dolomite minerals. Finally, we use a Debye-Waller model to calculate atomic displacements as a function of temperature from the vibrational spectroscopic data, for comparison with X-ray data.

Samples and Experimental Methods

Natural end-member single crystals of calcite, magnesite, dolomite and aragonite from private collections were used for this study. They were all characterized by X-ray diffraction, transmission electron microscopy (TEM) and Raman spectroscopy. Comparison with previous published results indicates that the minerals are indistinguishable from end-members. Some twins and isolated dislocations were observed in all four phases in the TEM study.

High-pressure (HP) and high-temperature (HT) Raman spectra were obtained by using either a heating stage or a diamond anvil cell (DAC) and a multichannel Raman microprobe (XY from DILOR) equipped with a confocal stage which enhances the signal to noise ratio by eliminating most of the parasite light due for instance to sample and diamond fluorescence or black-body thermal emission in high-temperature measurements. The light was collected in a 180° backscattering geometry through Leitz UTK 40 (with the DAC, focal distance 14 mm, numerical aperture 0.32) or Olympus ULWD 50 (with the heating stage, focal distance 8 mm and numerical aperture 0.63) objectives. At the sample the focused laser spot was less than 5 μm in diameter. The Raman light is focused into a spectrograph equipped with a 1200 gr/mm grating and analyzed by a CCD detector (EGG). Typical slit widths were between 70 and 100 μm. The spectral resolution was around 10 μm, giving a bandpass of approximately 2.5 cm^{-1}. The Raman spectra were obtained from accumulations lasting from 25 to 300 s for the HT and HP runs, respectively. Peak positions were estimated to within ± 1 cm^{-1}. The 514 or 488 nm lines of an argon ion laser were used at an output power ranging from 500 to 1500 mW. Only 5 to 10% of this power reaches the sample, due to absorption in the objectives, diamonds or heating-stage windows.

For the high-pressure experiments, 10 to 50 μm sized mineral chips, ruby grains for pressure calibration and KBr as pressure medium were introduced in a 200-μm hole of a stainless-steel gasket. Several 1–5 μm sized ruby chips were embedded in the KBr to check for pressure gradients. Pressure differences throughout the sample were less than 0.2–0.3 GPa below 10 GPa and never exceeded 1–2 GPa above 20 GPa. Raman spectra for a given pressure were collected on grains closest to the ruby chip used for pressure determination. KBr was used as a pressure medium in these experiments, because it is "softer" (gave rise to smaller pressure gradients in the cell) than the 1:4 ethanol-methanol mix which becomes solid and hard at around 10 GPa.

For the high-temperature spectra, unoriented (50 μm sized) grains were inserted in a Leitz 1350 heating stage. Temperatures were measured with a precision of 5–10 K with a Pt-PtRh 10% thermocouple and calibrated from the melting points of various pure compounds.

Spectra Under Ambient Conditions

The Raman spectra of the carbonates studied are well-known at ambient conditions. The optical vibrations can be separated into internal vibrations of the CO_3 group (lying between 700 and 1500 cm^{-1}) and external or lattice vibrations involving translation and librations of the CO_3 groups relative to the Ca or Mg atoms (100–500 cm^{-1}) (Couture 1947; White 1974). The vibrations of the "free" CO_3 group (ν_1: symmetric stretch; ν_3 asymmetric stretch; ν_2: out-of-plane bend; ν_4 in-plane bend) have been observed and assigned in the IR and Raman spectra of the carbonates of both rhombohedral and orthorhombic symmetry (White 1974). The site symmetry of the CO_3 group is determined by the cation environment and modifies the selection rules (i.e. the number of bands observed), and the frequencies to a small extent, when compared with the free group.

Calcite and Magnesite

Calcite and magnesite belong to the space group $R\bar{3}c$ and the symmetry analysis shows that there are 30 vibrations, which can be classified as:

$1A_{1g} + 4E_g$ (Raman active)
$4A_{2u} + 5E_u$ (Infrared-active)
$1A_{2u} + 1E_u$ (acoustic)
$3A_{2g} + 2A_{1u}$ (inactive modes)

The five expected Raman bands of both minerals are easily observed in our spectra with wavenumbers to within 1 cm^{-1} of those reported in earlier studies (Figs. 1 and 3). Three Raman bands are assigned to internal vibrations of the CO_3 groups: ν_1 (1084, 1094 cm^{-1}); ν_3 (1434, 1444 cm^{-1}) and ν_4 (711, 738 cm^{-1}). The first over-

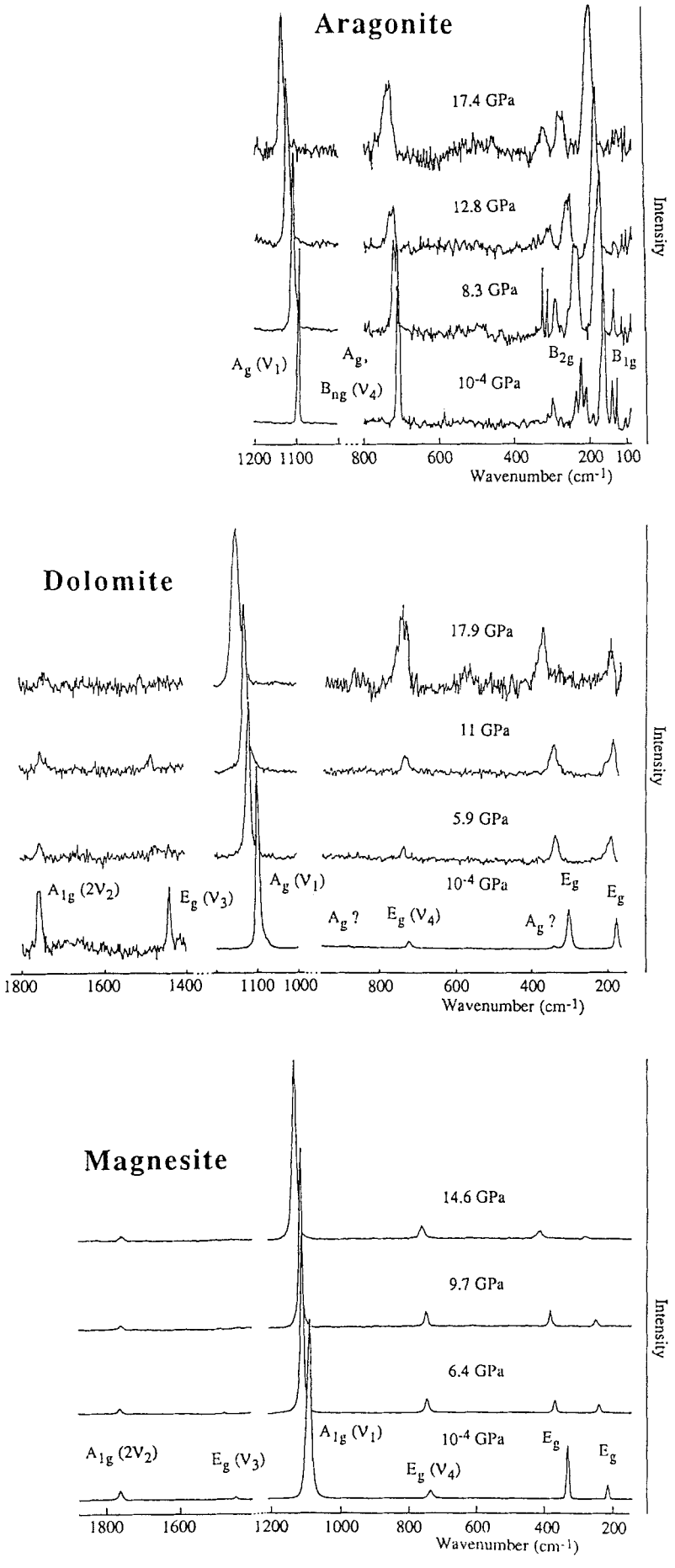

Fig. 1. Typical high-pressure Raman (at room temperature) spectra for magnesite, dolomite and aragonite. The band assignments of the room pressure and temperature spectra are discussed in the text

tone of an IR-active internal node (v_2) is also observed, at 1748 cm^{-1} and 1762 cm^{-1} for the two structures, respectively.

Dolomite

Dolomite belongs to the $R\bar{3}$ space group and the symmetry analysis shows that there are 30 vibrations, which can be classified as:

$4A_g+4E_g$ (Raman active)

$5E_u+5A_u$ (IR active)

$1E_u+1A_u$ (acoustic)

The slight symmetry differences with calcite induce only minor differences in the Raman spectra. As discussed previously by several authors, removal of the two fold axes and the glide plane on passing from the $R\bar{3}c$ (calcite) to the $R\bar{3}$ (dolomite) structure is interesting, in that the three silent modes of A_{2g} symmetry in calcite become Raman active (A_g symmetry) for dolomite (Couture 1947; White 1974; Nicola et al. 1976). The structural perturbations between calcite and dolomite are small, with the result that the additional A_g modes are weak, and should lie close in frequency to their silent counterparts in calcite and magnesite (Nicola et al. 1976). Nicola et al. (1976) have assigned these "additional" A_g modes at 1125, 343, and 273 cm^{-1}, in a single crystal study of dolomite. We observe the A_g peak at 335 cm^{-1}, assigned to a motion of the CO_3 groups parallel to the c axis, consistent with Nicola et al. (1976), and with Couture (1947) and White (1974). We find no evidence for the 1125 cm^{-1} nor the 273 cm^{-1} peaks reported by Nicola et al. (1976), but instead observe a weak peak at 880 cm^{-1} (Figs. 1 and 3). From IR studies, a v_2 internal mode of A_g symmetry should lie in this frequency range (Couture 1947; White 1974), and we propose that the 880 cm^{-1} peak is the second dolomite A_g mode corresponding to a silent A_{2g} of calcite. The lowest frequency A_{2g} mode of calcite was measured at 172 cm^{-1} by inelastic neutron scattering, and calculated at 210 cm^{-1} for calcite and 287 cm^{-1} for magnesite (Cowley and Pant 1973; Plihal 1973; Plihal and Schaak 1970). We have not observed the analogue of this mode in dolomite. In conclusion, 7 of the 8 expected fundamental Raman modes have been observed, among which the four expected bands corresponding to internal modes are present in our spectra. The overtone of the v_2 mode appears at 1750 cm^{-1}.

Aragonite

Aragonite belongs to space group *Pnma* and factor group analysis predicts 60 modes which can be classified as follow:

$9A_{1g}+6B_{1g}+6B_{2g}+9B_{3g}$ (Raman active)

$8B_{1u}+8_{2u}+5B_{3u}$ (IR active)

$6A_{1u}$ (inactive)

$1B_{1u}+1B_{2u}+1B_{3u}$ (acoustic)

30 Raman nodes are expected. All the corresponding bands have been observed by Frech et al. (1980). We have recorded several Raman spectra with different crystal orientations. Strong fluorescence of the sample and polarization effects have precluded the observation of all the modes. However at least 20 modes have been identified in our ambient spectra. Only 6 or seven modes have been unambigously tracked under pressure and temperature (Figs. 1 and 3). 9 internal modes of the CO_3 group should be observed in the Raman spectra (Frech and Wang 1980) (Fig. 1): $4v_4$ (700–720 cm^{-1}), $2v_2$ (850–910 cm^{-1}), $2v_3$ (1460–1575 cm^{-1}) and $1v_1$ (1085 cm^{-1}).

Assignment of Lattice Modes in Calcite, Dolomite and Magnesite

The assignment of the two low frequency Raman lattice modes of rhombohedral carbonates to translational or librational motions is still not clearly established (Bischoff et al. 1985). Based on an analysis of the IR and Raman spectra of calcite, Cabannes (1942) assigned the lower frequency component to libration, and the higher frequency mode to the hindered translation. This assignment has been accepted in more recent studies (Couture 1947; White 1974), although as noted by Krishnamurti (1957), both modes have probably mixed character. Rousseau et al. (1968) carried out a $^{14}N/^{15}N$ isotopic study on isostructural $NaNO_3$. These authors observed an isotopic shift of the lower frequency mode and none for the higher frequency mode, and concluded that the lower frequency peak should be assigned to the translational mode, and that there was little vibrational coupling between this and the libration. Bischoff et al. (1985) adopted this assignment for the purposes of description, although they recognised that significant mixing might occur for carbonates (as had been noted by Rousseau et al. 1968). In fact, the observed isotopic shifts for $NaNO_3$ do not necessarily lead to an unambiguous identification of the translation and libration modes, because of the Teller-Redlich rules for isotope shifts in system with coupled vibrational modes of the same symmetry species (Herzberg 1945).

In this context, it is extremely interesting to note the analogy between carbonates and the corresponding metal oxides with the NaCl (B1) structure. The calcite structure can be described as a distorted version of B1, with the CO_3^{2-} groups replacing the O^{2-} ions within the structure (Reeder 1983). We have made an error in the calculations. This sentence must be removed. It does not alter what follows because these results are not used. This permits an analogy to be made between the triply degenerate optic mode of the B1 structure, and the $A_{2u}+E_u$ (or $A_{2g}+E_g$) modes of the calcite minerals, derived from relative vibrations of the metal against the carbonate ion sublattices. It is interesting to note that, for the Raman active E_g vibrations, the metal cations do not participate in the translational mode, which becomes a displacement of the CO_3 groups against a stationary ca-

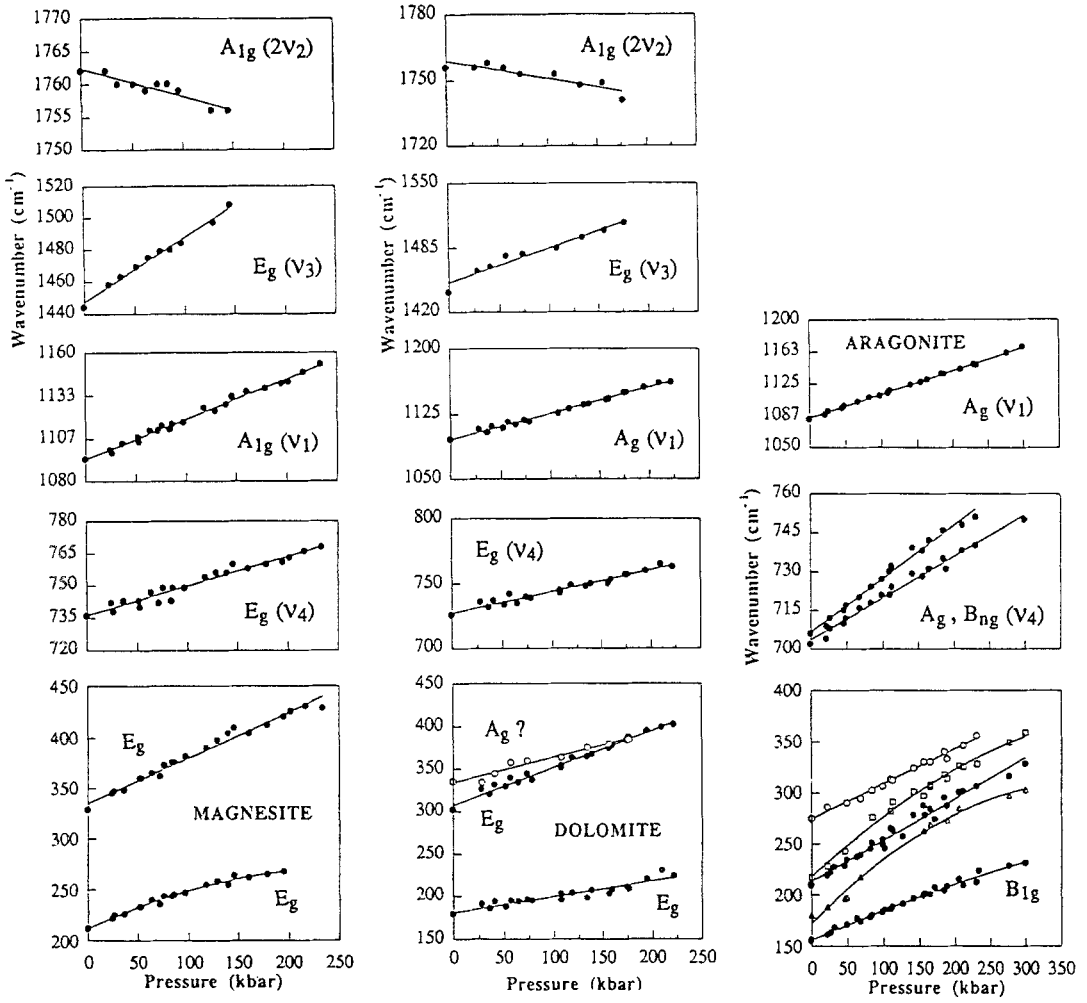

Fig. 2. Pressure dependence of the vibrational frequencies. The experimental uncertainty in measured peak positions lies within the size of the symbol. Magnesite (left), dolomite (middle) and aragonite (right)

tion sublattice. The optic mode frequencies (ν_{TO}) for CaO and MgO occur at 286–295 cm^{-1} and 401–403 cm^{-1}, respectively (Ross 1972; Farmer 1974). One $E_u - A_{2u}$ pair in calcite occurs at 297 and 303 cm^{-1}, and there are E_g and A_{2g} modes at 283 and 309 cm^{-1} (Cowley and Pant 1973; White 1974). In magnesite, there are E_u and A_{2u} modes at 356 and 362 cm^{-1}, and a Raman active E_g mode at 329 cm^{-1}. The analogy between these low frequency lattice modes and the optic mode for the B1 oxide is excellent in the case of calcite and, although less so for magnesite, is at least suggestive. We propose that this observation lends strong support for the assignment of the higher frequency lattice mode observed in the Raman spectrum of calcite, the E_g vibration at 283 cm^{-1}, along with the corresponding E_u, A_{2u} and A_{2g} modes, to the hindered translation. This is consistent with the earlier mode assignments for calcite (Cabannes 1942; Couture 1947; White 1974), and also with our analysis of the Debye-Waller factor, discussed below. Although the assignment is less clear for magnesite, the fact that the Raman-active lattice mode at 329 cm^{-1} lies much closer to the optic mode frequency in MgO than does the lower frequency lattice vibration (213 cm^{-1}) indicates that it is better assigned to the translational mode than to the libration. We regard this as a useful working assignment in this study: however, we recognise that all of the low frequency lattice modes of the same symmetry species are likely to be coupled to some extent. In addition, further coupling between modes of different symmetry species may occur through anharmonic effects, discussed in detail in a later section.

High-Pressure Raman Data

Spectra were recorded at room temperature and at pressures up to 30 GPa for aragonite, 25 GPa for magnesite, 23 GPa for dolomite. For calcite, the data of Liu and Mernagh (1990) have been used for intercomparison purposes. Typical Raman spectra at pressures are reported in Fig. 1. The pressure-induced shifts are reported in Fig. 2 and Table 1. Kraft et al. (1991) have published the IR (up to 40 GPa) and Raman (up to 22 GPa) spectra of aragonite and the Raman (up to 23 GPa) spectra of dolomite. Collerson et al. (1991) have reported Raman data on magnesite up to 20 GPa. Recent measurements on calcite from our laboratory are also included in Table 1. They are in agreement with those of Liu and Mer-

Table 1. Pressure shifts of the Raman modes of calcite, magnesite, aragonite and dolomite

Aragonite		Calcite		Dolomite		Magnesite	
ν_i cm^{-1}	$\partial\nu_i/\partial P$ cm^{-1}/kbar	ν_i cm^{-1}	$\partial\nu_i/\partial P$ cm^{-1}/kbar	ν_i cm^{-1}	$\partial\nu_i/\partial P$ cm^{-1}/kbar	ν_i cm^{-1}	$\partial\nu_i/\partial P$ cm^{-1}/kbar
155	0.30(3)−0.5(2) $10^{-4}P$ *0.27(2)*	156	0.25(3) *0.23(3)*	178	0.18(2) *0.14(2)*	213	0.46(4)−4.4(3) $10^{-4}P$ *0.44*
180	0.72(3)−4.7(4) $10^{-4}P$ *0.34(6)*						
209	0.40(4) *0.33(5)*	281	0.53(4) *0.60(5)*	300	0.44(3) *0.44(3)*	329	0.45(3)
217	0.66(4)−3.3(3) $10^{-4}P$						
275	0.34(3)			335	0.29(2)		
702	0.16(3) *0.18(1)*	711	0.22(2) *0.17(3)*	724	0.16(3) *0.11(2)*	738	0.14(2) *0.16*
710	0.20(3)			880	?		
1084	0.27(3) *0.20(1)*	1085	0.59(4) *0.30(3)*	1097	0.29(3) *0.35(3)*	1094	0.25(3)
1463	?	1434	0.90(5) *0.75(5)*	1439	0.35(3)	1444	0.40(4)
1575	?	1748	*−0.10(4)*	1750	−0.079(5)	1762	−0.042(4)

The data for calcite are from Liu and Mernagh (1990). The numbers in italics represent the shifts measured by Kraft et al. (1991) for dolomite and aragonite and Collerson et al. (1991) for magnesite. For calcite the data are from Liu and Mernagh (1990) and those in italics represent the shifts measured in our laboratory

nagh (1990). These studies reached the same conclusions, namely that aragonite, magnesite and dolomite have no pressure-induced phase transitions at room temperature in the pressure range explored, in contrast with calcite (Fong and Nicol 1971; Gillet et al. 1988; Liu and Mernagh (1990). The pressure shifts found in the present study are in general agreement with those measured in previous works (Table 1). However, we report for the first time the pressure shifts of the less intense ν_3 and $2\nu_2$ Raman modes of magnesite and dolomite, the shift of an additional lattice mode of dolomite at 335 cm^{-1}, the shift of the $2\nu_2$ Raman mode of calcite and finally the shifts of two ν_4 modes at around 700 cm^{-1} in aragonite. It must also be noticed that our data show a measurable decrease of the $(\partial\nu_i/\partial P)_T$ values with pressure for 3 Raman-active lattice modes of aragonite and one lattice mode of magnesite. This was not observed by Kraft et al. (1991).

All the modes increase in frequency with pressure, with the exception of the overtones of the ν_2 internal modes of CO_3 in magnesite, calcite and dolomite (at around 1750 cm^{-1}). This negative shift in pressure of the out-of-plane bending mode of the CO_3 group has already been observed in aragonite (Kraft et al. 1991) and thus seems to be general in carbonates. This is consistent with the negative anharmonicity for the ν_2 mode ($\Delta(\nu_{0-2}-2\nu_{0-1})=-4$ and -10 cm^{-1} for calcite and magnesite, respectively). Some reasons for this have been discussed by Kraft et al. (1991). The relative changes in frequency $(\partial \ln \nu_i/\partial P)_T$ (Fig. 3) of the internal modes of the CO_3 groups are lower than those of the lattice modes.

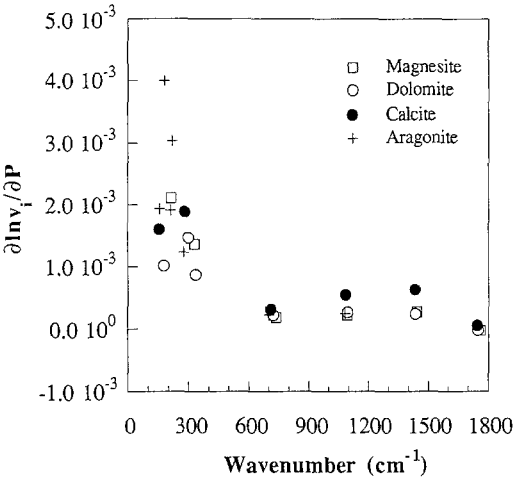

Fig. 3. Relative changes in internal and lattice vibrational frequencies with pressure $(\partial \ln \nu_i/\partial P)_T$ for calcite, dolomite, aragonite and magnesite

Ross and Reeder (1992) have shown that the crystal bulk moduli of ankerite and dolomite are very close to those of the CaO_6, MgO_6, and FeO_6 octahedra, CaO_6 being slightly more compressible. The CO_3 group appears to be insensitive to pressure increase at least up to 4–5 PGa. Hence, the difference in the $(\partial \ln \nu_i/\partial P)_T$ values between internal and lattice modes, at least for calcite, dolomite and magnesite, can be related in a first approximation to the greater incompressibility of the CO_3 groups when compared with the calcium or magnesium polyhedra (Ross and Reeder 1992). For aragonite

a similar trend between lattice and internal modes is also observed and may be related to a similar differential compression between the CO_3 group and the CaO_6 octahedron.

We have shown in previous work that there is a general relation between $(\partial \ln \nu_i/\partial P)_T$ values for lattice modes and the bulk modulus, with a small pressure shift for phases having the largest bulk modulus (Gillet et al. 1992). However, this correlation does not appear to hold from mode to mode for the carbonates studied here. The bulk moduli for calcite, dolomite and magnesite are, respectively, 73, 94 and 112 GPa (Martens et al. 1982; Ross and Reeder 1992). However, the pressure shift for the lowest frequency lattice mode is largest for magnesite, and smaller for both calcite and dolomite, whereas the pressure shift for the higher frequency lattice mode is very similar for all three phases (Table 1). This is discussed in detail below. The frequency changes of the internal modes of the CO_3 group are quite similar in magnesite, dolomite and aragonite, and differ significantly from those of calcite (Liu and Mernagh 1990). There are two possible explanations to account for this observation. First of all, if the internal mode frequency shifts are related to the C–O bond compressibility, then the C–O bond must be two times more compressible in calcite than in the other two phases. However, it seems more likely that the differing behaviour of the internal modes between calcite and the other carbonate phases is related to changes in the local cation environment symmetry, and to dynamical effects like the 11° rotation of the CO_3 groups accompanying the calcite I-calcite II transition (Merrill and Basset 1975). Finally, our own measurements on calcite agree with those of Liu and Mernagh (1990) for all but one mode (1085 cm^{-1}) for which we report a shift very similar to that observed in the other studied carbonates. It is thus possible that the behaviour of the CO_3 groups is similar in all the studied carbonates. Kraft et al. (1991) have also interpreted their high-pressure Raman data in terms of possible structural changes upon compression, in particular the negative pressure shift of the ν_2 modes.

For aragonite the $(\partial \ln \nu_i/\partial P)_T$ of the internal modes are similar to that of the $R\bar{3}c$ carbonates and may therefore account for a similar behaviour of the CO_3 during compression.

High-Temperature Raman Data

Spectra were recorded up to the temperatures at which decarbonation of the samples under air partial pressure of CO_2 took place: $\approx$800° C for calcite, $\approx$700° C for dolomite and $\approx$600° C for magnesite. Decarbonation is detected in the spectra by a sudden disappearance of the strongest Raman bands. For aragonite spectra were recorded up to 450° C, a temperature at which the transformation into calcite becomes very rapid (Gillet et al. 1987). In order to check the data and their reproducibility, care was taken to make at least two runs and to record in each case spectra during heating and, if no decarbonation had occurred, during cooling. For calcite, dolomite and magnesite all the Raman active modes observed at ambient conditions have been followed at temperature. For aragonite, only the strongest bands have been studied.

Typical high-temperature spectra are shown in Fig. 4. All the Raman modes show a wavenumber decrease with increasing temperature, with the exception of the ν_4 in-plane bend of the CO_3 groups which remain unchanged (or are only slightly affected by temperature), within experimental uncertainty. Several modes exhibit non-linear shifts (Fig. 5). The temperature $(\partial \nu_i/\partial T)_P$ shifts of the modes of the four minerals are reported in Table 2. For calcite and aragonite the present data are in good agreement with those of the earlier study of Salje and Viswanathan (1976).

The following general remarks can be made. From Table 2 and Fig. 6, it is seen that the individual relative temperature-induced frequency shifts $(\partial \ln \nu_i/\partial T)_P$ of the Raman modes are an order of magnitude lower for the internal modes (ν_1, ν_3, ν_2 and ν_4) of the CO_3 group than for the lattice modes. Moreover the lattice modes of calcite are more sensitive to increasing temperature than are those of dolomite and magnesite, in contrast with the internal modes, which generally behave in a similar manner with temperature in all three minerals.

Table 2. Temperature shifts of the Raman modes of calcite, magnesite, aragonite and dolomite

Aragonite		Calcite		Dolomite		Magnesite	
ν_i cm^{-1}	$\partial \nu_i/\partial T$ $cm^{-1}/°C$	ν_i cm^{-1}	$\partial \nu_i/\partial T$ $cm^{-1}/°C$	ν_i cm^{-1}	$\partial \nu_i/\partial T$ $cm^{-1}/°C$	ν_i cm^{-1}	$\partial \nu_i/\partial T$ $cm^{-1}/°C$
155	−0.027(3)	156	−0.028(3)	178	$-0.019(2)-3.5(3)\ 10^{-6}T$	213	$-0.009(2)-2.6(2)\ 10^{-5}T$
180	−0.024(3)						
209	−0.041(4)	281	−0.040(3)	300	$-0.032(3)-1.96(5)\ 10^{-5}T$	329	$-0.019(3)-2.5\ 10^{-5}T$
254	−0.020(3)			335	$-0.019(2)-7.8(5)\ 10^{-5}T$		
702	0	711	−0.004(1)	724	$-0.0021(5)-1.7(3)\ 10^{-5}T$	738	0
710	−0.015(3)			880	0		
1084	−0.015(2)	1085	$-0.0040(2)-1.40(5)\ 10^{-5}T$	1097	$-0.0064(4)-1.6(3)\ 10^{-5}T$	1094	$-0.0035(3)-3.1(2)\ 10^{-5}T$
1463	−0.022(3)	1434	$-0.025(3)+2.9(3)\ 10^{-5}T$	1439	$-0.035(3)+4.1(2)\ 10^{-5}T$	1444	$-0.030(3)+5.5(2)\ 10^{-5}T$
1575	−0.031(3)	1748	$-0.0053(5)-2.3(2)\ 10^{-5}T$	1750	$-0.0013(2)-1.60(4)\ 10^{-5}T$	1762	−0.026(3)

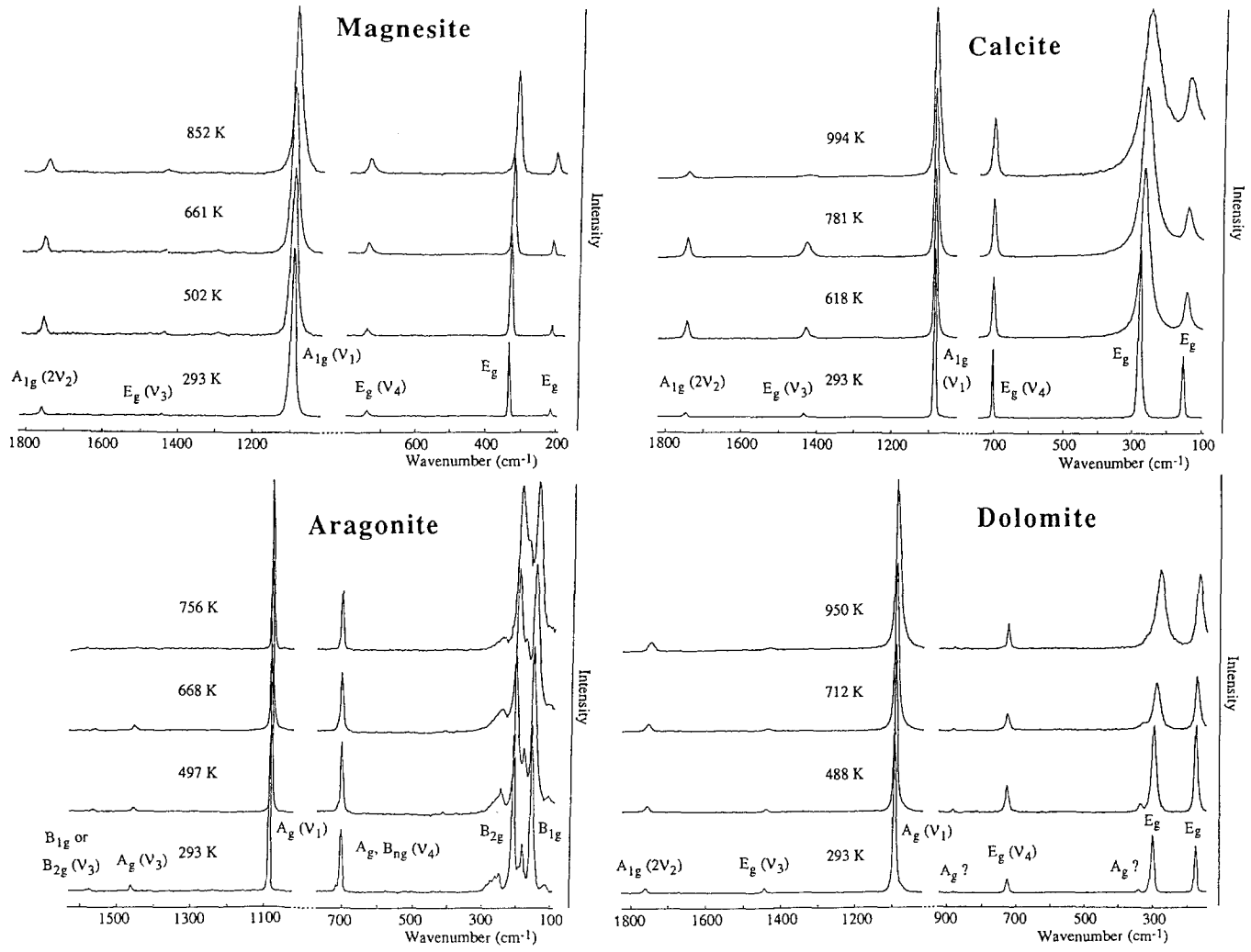

Fig. 4. Typical high-temperature Raman (at room pressure) spectra for calcite, dolomite, magnesite and aragonite. The band assignments of the room pressure and temperature spectra are discussed in the text.

As noted earlier, it is often assumed that the changes in vibrational frequency can be simply related to changes in bond length or polyhedral volume (e.g. Gillet et al. 1992). The high-temperature X-ray data of Markgraf and Reeder (1985) and Reeder and Markgraf (1986) give very similar coefficients of thermal expansion for the Ca−O and Mg−O bonds and CaO_6 and MgO_6 volume polyhedra. However the temperature shifts (both absolute and relative) of the lattice modes are significantly higher in calcite than in magnesite and dolomite. The X-ray data indicate that the distorsion of the octahedra increases at a markedly higher rate in calcite than in the two other carbonates. The increasing distorsion in calcite is due to a shortening of the O−O distance in the basal plane of the CaO_6 octahedra. The presence of Mg seems to hinder this distorsion increase in both magnesite and dolomite. It is therefore likely that the large variations with temperature of the amplitudes and frequencies of the CO_3 librations and translations, and the increase of the CaO_6 polyhedral distorsion in calcite, are closely related. In dolomite and magnesite the changes in frequency with temperature are quite similar and, can be related to a similar volume change of the CaO_6 and MgO_6 octahedra, without significant increase in polyhedral distorsion. Thus, the excess shift in calcite can be related to the strong increase in octahedral distorsion, associated with a strong anharmonic increase of vibrational amplitudes for CO_3 librational degrees of freedom, eventually driving the rotational order-disorder transition from $R\bar{3}c$ to $R\bar{3}m$ at higher temperatures (Megaw 1970; Markgraf and Reeder 1985; Reeder and Markgraf 1986; Redfern et al. 1989; Dove and Powell 1989).

From the high temperature X-ray structure refinements of Markgraf and Reeder (1985) and Reeder and Markgraf (1986), only a very small increase of the C−O bond length with temperature is observed: less than 0.4% between 300 and 800 K in magnesite and 300 and 900 K in dolomite, and about 1.5% in calcite between 300 and 1000 K. The frequency change with temperature of the symmetric stretching motion (ν_1) is of the same order for the three rhombohedral carbonates (0.4%), so that the greater apparent coefficient of thermal expansion of the C−O bond length in calcite is not simply reflected in the C−O stretching vibrational frequency changes with temperature. The ν_4 modes are only slightly affected by temperature, and significant frequency shifts

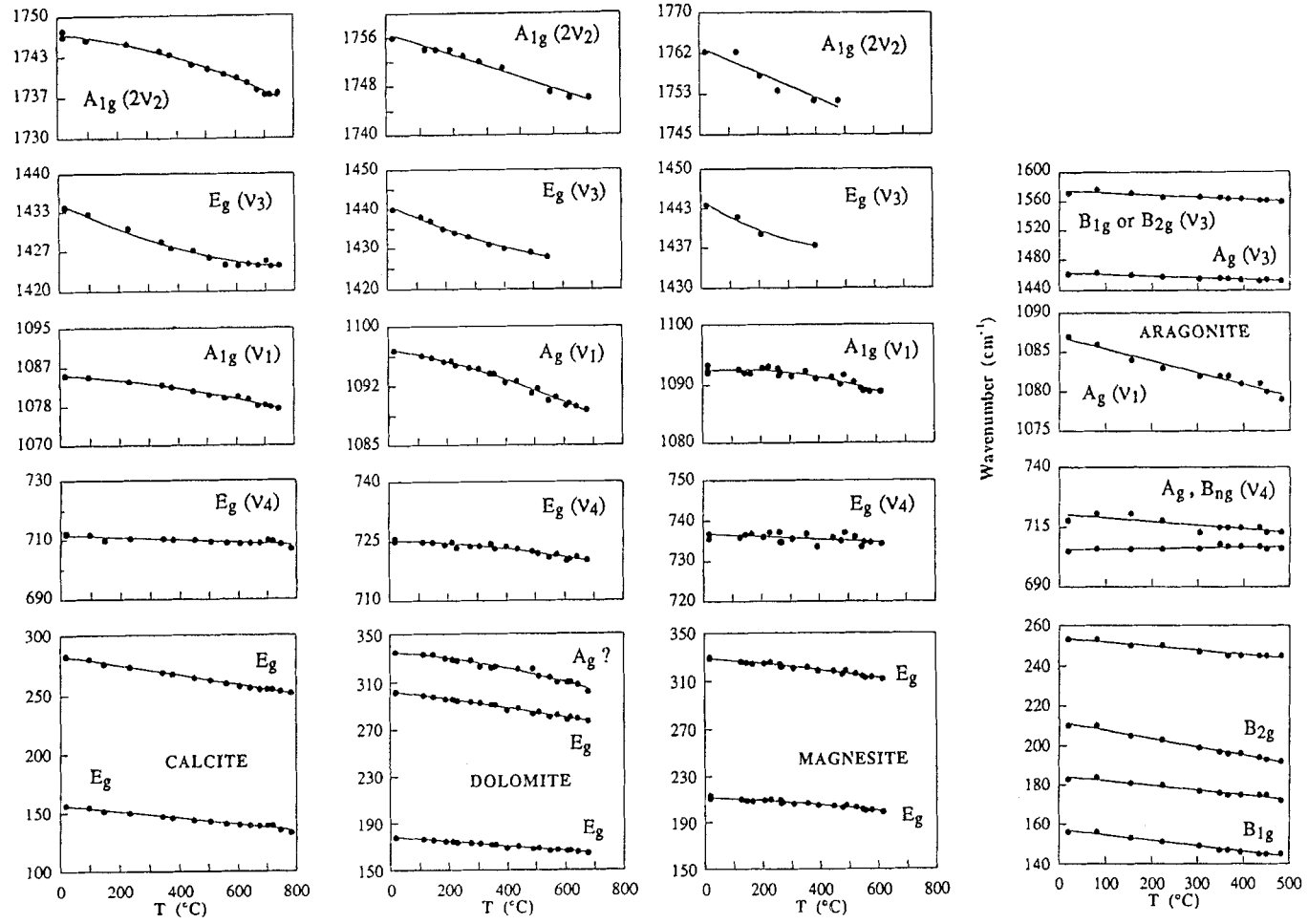

Fig. 5. Temperature dependence of the vibrational frequencies: calcite, dolomite, magnesite and aragonite. The experimental uncertainty in measured peak positions lies within the size of the symbol

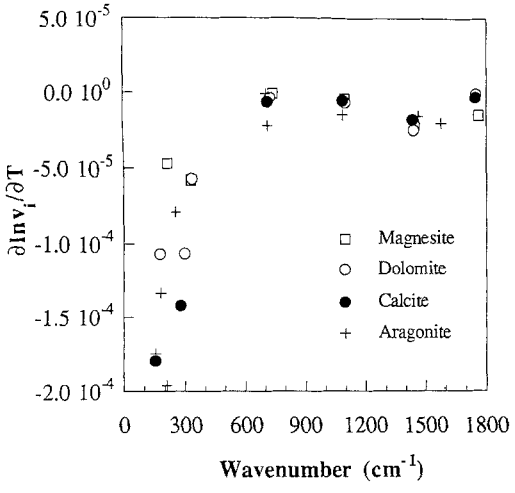

Fig. 6. Relative changes in internal and lattice vibrational frequencies with temperature $(\partial \ln \nu_i/\partial T)_P$ for calcite, dolomite, aragonite and magnesite

are only observed in calcite and dolomite. This may be linked to changes in distorsion of the MO_6 octahedral groups with temperature, which are pronounced in calcite, small in dolomite and absent in magnesite (Markgraf and Reeder 1985; Reeder and Markgraf 1986).

For aragonite, high-temperature X-ray refinements are not yet available. In addition, detailed assignment of the nature of the low frequency vibrational modes has not been carried out. However, most of the Raman-active lattice modes can be generally assigned to either pure librational, translational or mixed modes. Using arguments based on relative band intensities, Couture (1947) has attributed the two most intense modes at 155 and 208 cm^{-1} to librational motions of the CO_3 groups. Whatever the true mode assignment, it appears that most of the lattice modes are as temperature-dependent as those in calcite. This could indicate that the translational and librational amplitudes of the CO_3 groups are as important as in calcite. These enhanced amplitudes may therefore reflect progressive rotational disordering preceeding the aragonite to calcite transition. The internal modes of the CO_3 group are more sensitive to temperature than the corresponding modes in calcite, dolomite and magnesite. The greater temperature-induced shift of the ν_1 mode could reflect a greater expansion of the C–O bond length with temperature, although the discussion in the previous paragraph suggests that stretching mode frequencies may not simply be related to C–O bond length. Another interesting feature concerns the ν_4 modes at 712 and 702 cm^{-1}. The frequency separation

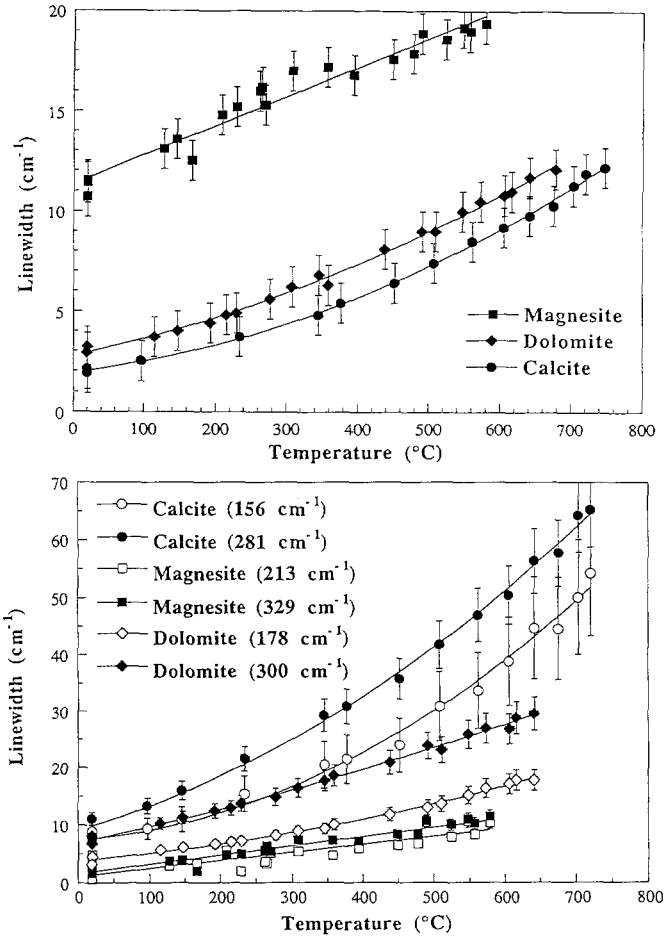

Fig. 7. Temperature dependence of the line widths of the Raman-active modes of calcite, dolomite and magnesite. Upper graph is for the ν_1 modes of CO_3^{--}

between these peaks results from site group splitting (White 1974). The 702 cm^{-1} mode does not shift with temperature, whereas the 712 cm^{-1} peak decreases in frequency with temperature. As a consequence, the site group splitting decreases with temperature. This can be interpreted as due to a symmetry increase of the local crystal field surrounding the CO_3 group, or by a decrease in distorsion of the CO_3 group itself.

The temperature evolution of the linewidths of the Raman modes of calcite, dolomite and magnesite are shown in Fig. 7. In calcite, the linewidths of the lattice modes increase more rapidly with temperature than those for dolomite and magnesite. At temperatures above 650 K, the linewidths of the lattice modes of calcite exhibit a strong non-linear increase with temperature. Unlike the frequency shifts, the linewidths of the high-frequency modes corresponding to internal vibrations of the CO_3 group do show some differences among the three rhombohedral carbonates. The linewidths at ambient conditions in dolomite and calcite are much smaller than that in magnesite. In addition, the evolution of the linewidths with temperature is non linear in calcite and dolomite, and nearly linear in magnesite.

It is interesting to note the similarity in behaviour of the low frequency lattice modes of calcite with temperature, and those of the isostructural phase $NaNO_3$. Like calcite, this phase undergoes a tricritical phase transition at 549 K (1260 K for calcite), associated with orientational disordering of the NO_3 groups about their three-fold axes (Bréhat and Wyncke 1985; Schmahl and Salje 1989; Redfern et al. 1989; Dove and Powell 1989). For the low frequency infrared- and Raman-active translational and libration vibrations, the mode frequencies decrease, and Raman linewidths and infrared mode damping parameters increase, regularly with temperature in a manner consistent with cubic anharmonicity associated with normal lattice thermal expansion, to a temperature approximately 100 K below the transition temperature (Shen et al. 1975; Neumann and Vogt 1978; Bréhat and Wyncke 1985). Above this temperature, Bréhat and Wyncke (1985) noted an anomalous increase in the damping parameters of the low frequency lattice modes, especially the A_{2u} vibrations derived from hindered translation and libration of the NO_3 groups, which they ascribed to an increasing contribution of an additional relaxational mode to the spectrum, precursor to the order-disorder transition. This is accompanied by an increased intensity in the Rayleigh wing observed in Raman spectroscopy, and the onset of a central mode in the Brillouin spectrum (Neumann and Vogt 1978; Yasaka et al. 1985).

Our observations for calcite suggest identical behaviour in the lattice mode region at high temperature. Up to approximately 400° C (673 K), the variation in Raman linewidths is quasi-linear, consistent with simple volume thermal expansion associated with a cubic anharmonicity term (Fig. 7). Above this temperature, there is an anomalous increase in linewidth, suggesting additional anharmonic terms associated with the relaxational mode. The variation in mode frequencies with temperature is characterized by strong curvature in this region, and an additional anomaly is observed in the frequency shifts near 700° C, close to the phase transition temperature (Salje and Viswanathan 1976; this work, Fig. 5). These changes are accompanied by an increase in intensity of the Rayleigh wing above 780 K. At the same time, we observe departures from linearity in the temperature behaviour of some of the high frequency internal modes, as observed by Bréhat and Wyncke (1985) for $NaNO_3$. These observations are consistent with increasing excitation of the relaxational degree of freedom of three-fold axis libration of the CO_3 groups, premonitory to the rotational order-disorder transition. The high temperature behaviour of dolomite and magnesite is much more regular, although there does appear to be an onset of anomalous broadening above approximately 700 K for dolomite, perhaps accompanied by a slight increase in intensity of the Rayleigh wing (Fig. 4). This could suggest that a similar rotational order-disorder transition might occur in dolomite at higher temperature than that in calcite. The difference in anharmonic behaviour of these and other calcite structures is examined in more detail in the following section.

Raman Mode Frequencies vs Structural Parameters

The differences in linewidth behaviour with temperature between calcite, dolomite and magnesite indicate differ-

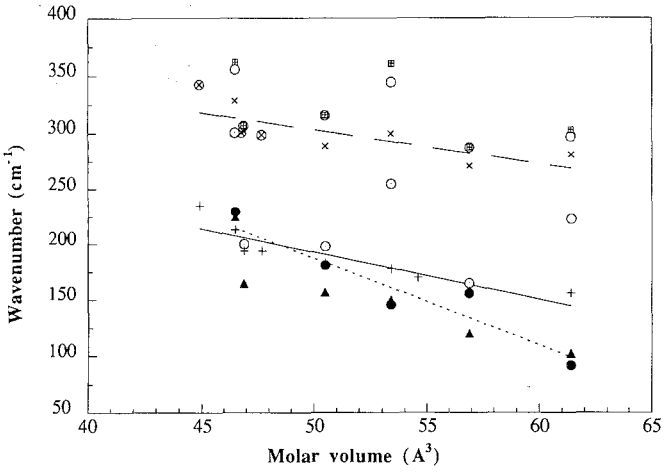

Fig. 8. Raman and IR lattice mode frequencies (translational and librational modes) for different rhombohedral carbonates as a function of molar volume. Data taken from White (1974), Rutt and Nicola (1974), and this work. The mode numbering scheme and symmetry assignments are those of White (1974)

ences in mode anharmonicites between the three carbonates, and it is interesting to explore possible structural reasons for this. Several authors have observed regular trends in the variation of lattice modes for calcite and dolomite structures with compositional and structural parameters (Rutt and Nicola 1974; Bischoff et al. 1985). We can use these trends to begin to understand the variation of lattice mode frequencies and anharmonicities with composition within these carbonate structures.

The lattice modes can be separated into three types, depending on the character of the atomic displacements involved. First, one set of modes are associated with hindered rotation of the CO_3 groups about their three-fold axes. This gives rise to two modes, of A_{2u} (IR active) and A_{2g} (inactive) symmetry, labelled v_7 and v_{12} by White (1974). The second type also involves libration of the CO_3 groups, but about a plane normal to the three-fold axis, giving rise to the v_{10} and v_{14} modes (E_u and E_g symmetry). Finally, the remaining lattice modes involve relative translations of the metal and carbonate sublattices, related to the optic modes of the corresponding B1 structure, as discussed previously.

At temperatures below the onset of significant excitation of the relaxational mode associated with three-fold axis rotation of the CO_3 groups, the temperature dependence of the frequency shifts and linewidths of the lattice modes in calcite, and in dolomite and magnesite, can be understood by a simple cubic anharmonicity associated with volume thermal expansion (Bréhat and Wyncke 1985). In their high-temperature infrared emissivity study of calcite, Sakurai and Sato (1971) found that the anharmonicity of both lattice and internal modes were dominated by the cubic term at low temperatures. In their fit of anharmonic parameters, these authors find that the quartic anharmonicity term reaches 30% of the value of the cubic term by approximately 400° C, the temperature at which we observe significant curvature in the temperature-dependence of the Raman active lattice modes. For this reason, we might expect a simple dependence of the frequencies and linewidths of the Raman active lattice modes, and frequencies and damping coefficients of IR modes in calcite and dolomite structures, measured at low (ambient) temperature on the unit cell volume.

In Fig. 8, we plot the frequencies of the lattice modes measured for carbonates with the calcite and dolomite structures, as a function of the molar volume. There is a generally decreasing trend in frequency with increasing volume for all of the lattice modes, consistent with the idea expressed above. There is considerable scatter in the infrared modes, especially those in the 250–350 cm^{-1} range, which may be largely instrumental, but the Raman-active lattice modes (E_g(13) and E_g(14)), and two of the infrared modes (A_{2u}(7) and E_u(10)) show a nearly linear decrease in frequency with increasing volume. There are two additional interesting points to note in this figure. First, although we have fit the frequency variation for four of the lines by linear least squares regression, mainly as a guide to the eye, there is some evidence for strong curvature in some of the trends for the lowest volume structures. This is especially noticeable for the lower frequency Raman node (E_g(14)), but is also apparent for some of the other modes. This will be discussed below, when we compare the differences in $v(P)$ and $v(T)$ behaviour of calcite, dolomite and magnesite. Second, we note that the two Raman active lattice modes, with mixed translational and librational character, have similar slopes to the overall trend, whereas the lowest frequency infrared mode (A_{2u}(7)), due to three-fold axis libration of the CO_3 groups, has a steeper slope. We suggest that this may be due to an additional intrinsic anharmonicity associated with this mode, over that taken into account by consideration of the volume term alone.

As noted earlier, calcite undergoes a high-temperature phase transition associated with rotation of the CO_3 groups about their three-fold axes (Megaw 1970; Redfern et al. 1989; Dove and Powell 1989). The three-well potential energy function for this rotation might be considered to be a simple sinusoidal function, as a first approximation. This type of potential was considered in early assignments of satellite lines observed in infrared experiments at low temperatures (Hexter 1958; Schroeder et al. 1962), although the particular combination band assignments discussed have been superceded by later work (Hellwege et al. 1970). Such a potential function is inherently anharmonic. The degree of anharmonicity observed for a given degree of vibrational excitation is determined by the barrier height, relative to

the vibrational levels within the well. The barrier height is most affected by oxygen – oxygen repulsion between adjacent carbonate groups, hence by the carbon – carbon distance. This in turn is determined by the metal-oxygen distance, and the unit cell volume. Hence, one would expect a greater effect of the anharmonicity of the potential on the librational motion at a given temperature for calcite, with long M – O bonds (hence larger volume, and greater oxygen ... oxygen separation), than for magnesite, with shorter M – O bonds. If the form of the potential function remains constant between the different carbonates, lowering the barrier height will reduce the curvature at the bottom of the potential well, hence the vibration frequency. Thus, we expect that the largest volume structures should have the most anharmonic librations, with the lowest vibrational frequencies. We propose that it is this additional intrinsic anharmonicity of the librational motion which is responsible for the anomalously large dependence of the A_{2u} mode frequency on molar volume (Fig. 8).

The remaining types of lattice mode in the carbonate structures include the translational modes derived from the optic vibration of the B1 oxides ($A_{2u}+2E_u+E_g$), and the librations (E_u and E_g) derived from tilting the CO_3 groups. The high-temperature behaviour of the two E_g Raman modes in calcite indicates a high degree of anharmonicity, but only normal anharmonicity for magnesite. In addition, Sakurai and Sato (1971) have investigated the anharmonicity of three infrared active modes of calcite via high temperature emissivity measurements, including the low frequency E_u translational mode at 305 cm^{-1}. This mode has a damping coefficient $\gamma_j = 23.8$ cm^{-1} at room temperature, more than five times that of the higher frequency internal vibrations, and shows a rapid increase in anharmonic damping with increasing temperature. Because these modes do not belong to the same symmetry species as the intrinsically anharmonic three-fold axis libration discussed above, it is interesting to explore the origin of the anharmonicity in these low frequency Raman- and infrared-active modes.

Infrared reflectivity measurements have been carried out for the corresponding oxide phases CaO and MgO by Jacobson and Nixon (1968) and Piriou (1974). In contrast to the translational mode in calcite, the anharmonic damping coefficient for the oxides is much smaller: 7.6 cm^{-1} for MgO and 0.07 cm^{-1} for CaO. From this comparison, it is unlikely that the high degree of anharmonicity for the lattice modes in calcite is derived from the translational component. For the libration associated with tilting the carbonate groups, we can say little about the likely form of the potential for this mode in calcite structures, but it could well be intrinsically anharmonic, judging by the large thermal ellipsoids sub-parallel to the mode eigenvector (Megaw 1970; Markgraf and Reeder 1985). If not, then the high degree of intrinsic anharmonicity of the Raman active lattice modes, and the infrared active E_u translational mode, could be due to anharmonic coupling with the three-fold axis libration. In fact, in their high-temperature structural study of these minerals, Markgraf and Reeder (1985) describe the importance of coupled translation and three-fold axis libration in calcite, which would correspond to exactly this type of anharmonic coupling between these modes. It is of interest that Markgraf and Reeder (1985) find this type of coupled motion to be much less important for magnesite, which agrees with our findings, discussed in the following paragraph.

To further explore the behaviour of the low frequency lattice modes, we have plotted the frequency dependence of the E_g modes of magnesite, dolomite and calcite observed in our high-temperature and high-pressure measurements, as a function of unit cell volume (Fig. 9). We have used the unit cell volume V in this case, rather than the molar volume, in order to provide an expanded plot. For $V(T)$, we have used the high-temperature data of Markgraf and Reeder (1985) and Reeder and Markgraf (1986). To obtain $V(P)$, we have used a Murnaghan equation of state,

$$V(P) = V_0(1 + K_0'/K_0\, P)^{-1/K_0'}, \quad (1)$$

with $K_0 = 73$ GPa for calcite, 94 GPa for dolomite, and 122 GPa for magnesite (Martens et al. 1982; Ross and Reeder 1992), and assuming $K_0' = 4$ for all three phases. The lines drawn on Fig. 9 represent the variation of the

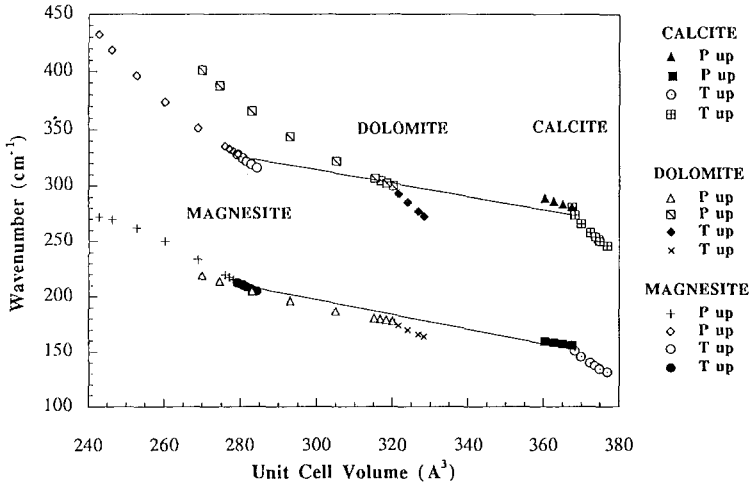

Fig. 9. Frequencies for Raman active lattice modes for calcite, dolomite and magnesite from high temperature and high pressure experiments (this study; Liu and Mernagh 1990) plotted against unit cell volume. The straight lines on this plot show the compositional volume dependence of these mode frequencies, from Fig. 8

E_g modes with volume at room pressure and temperature from the compositional studies described above. Compressing calcite at room temperature simply reverses the frequency trend for both modes along this line, as do the high-pressure frequency trends for dolomite and magnesite for the lower frequency E_g mode. We noted earlier that it is likely that this mode has more librational character than that at higher frequency. The higher frequency mode for magnesite increases more steeply with decreasing volume in the high-pressure experiments than expected from extrapolation of the compositional volume trend. This mode has more translational character, and is more sensitive to compression at smaller volume than the lower frequency librational mode. The high frequency mode in dolomite also increases in frequency with decreasing volume more rapidly than expected from the compositional volume trend, and is sub-parallel to the trend observed for magnesite. This could well reflect the stiffening of the translational mode against the magnesium sublattice in dolomite, rather than an averaged effect comparable with the compositional trend. The discussion is reversed for the high temperature volume behaviour of these modes. For magnesite, both modes follow a frequency trend close to that defined by the compositional volume expansion. This is consistent with the conclusions of Markgraf and Reeder (1985), that coupling between the tilting libration and translational modes, and the threefold axis libration, is much less important in magnesite than in calcite. For calcite, which lies at the large volume limit of the compositional expansion, both modes soften much more rapidly than expected from extrapolation of the compositional trend to larger volume. We propose that this is due to an additional (quartic) anharmonic coupling with the threefold axis libration, which is most important for the largest volume structures, as discussed earlier. Once more, the behaviour of the two modes in dolomite is different. The lower-frequency mode frequency decreases with increasing temperature, sub-parallel to the compositional volume trend. The higher frequency mode shows a similar large deviation from the compositional trend as does calcite. This might suggest that the higher frequency translational mode is more strongly coupled with the anharmonic three-fold axis libration in dolomite than is the lower frequency tilting librational mode. Reeder and Markgraf (1986) find that the degree of screw coupling, between the translational and three-fold axis libration degrees of freedom, is intermediate in dolomite between those of calcite and magnesite. From our results (Fig. 9), it is apparent that the intermediate behaviour of dolomite is due to the different degrees of coupling of the translational and tilting librations with the highly anharmonic three-fold axis libration.

White (1974) has discussed the variation of the internal modes of the CO_3 groups with composition for calcite and other carbonate structures. Apart from the ν_4 vibration, the trends are poorly defined, and are less easy to understand than those for the lattice vibrations. However, we can make some remarks concerning the difference in frequencies and linewidths for the ν_1 symmetric stretching vibration between calcite and magnesite. The value of the Raman active stretching frequency is determined by two major competing factors. First, as the strength of the M–O bond increases, the C–O bond strength is decreased, lowering the C–O stretching frequency. However, this is compensated by an increased contribution of the M–O stretching force constant to the vibration, with the opposite effect. Competition between these opposing effects is probably partly responsible for the relative constancy of the ν_1 stretching frequency for a wide range of carbonates (White 1974), and for the minor changes found within compositional series (Bischoff et al. 1985). The effect on the linewidths is, however, more easy to examine and understand. The ν_1 linewidth in magnesite is considerably larger than that for calcite (Fig. 7). Because the Mg–O bond is stronger than Ca–O, there is increased competition for the oxygen ion between carbon and the metal cation in magnesite compared with calcite, so we expect the C–O stretching vibration to be more anharmonic in $MgCO_3$ than $CaCO_3$. We propose that it is this increased anharmonicity which results in the increased linewidth for magnesite, relative to calcite.

Raman *Versus* X-ray Data at High Temperatures

Markgraf and Reeder (1985) and Reeder and Markgraf (1986) have pointed out that the amplitude of both rigid-body translation and libration of the CO_3 group increase with increasing temperature, calcite being by far more sensitive than dolomite and magnesite. In calcite, the larger amplitude of the libration has been interpreted as a precursor to rotational disorder of the CO_3 groups, before the $R\bar{3}c$ to $R\bar{3}m$ transition (Reeder and Markgraf 1986). Our high-temperature Raman results on the behaviour of the low frequency translational and librational lattice modes of calcite, along with those of the pioneering study of Salje and Viswanathan (1976), support this interpretation. Dove and Powell (1989) and Schmahl and Salje (1989) have recently applied Landau's theory for tricritical phase transitions to the $R\bar{3}c$ to $R\bar{3}m$ transition in calcite, using this rigid body model. In the following discussion, we investigate the relation between observed high temperature vibrational data, and the librational and translational motions inferred from X-ray refinements at high temperatures (Markgraf and Reeder 1985 and Reeder and Markgraf 1986).

Libration and Translation of the CO_3 Group

From high-temperature X-ray data, Markgraf and Reeder (1985) and Reeder and Markgraf (1986) have refined the rigid thermal motions (**TLS** parameters) of the CO_3 group in calcite, dolomite and magnesite. These parameters are, respectively, $T_{11}=T_{22}=\langle u_{11}^2\rangle$ describing the amplitude of translation of CO_3 within the (0001) plane, $T_{33}=\langle u_{33}^2\rangle$ describing the translation parallel to [0001], $L_{11}=L_{22}=\langle \phi_{11}^2\rangle$ for librations about axis within (0001), and finally $L_{33}=\langle \phi_{33}^2\rangle$ for librations around [0001]. Each of these T_{ii} or L_{ii} parameters is the sum

of the contributions of different optical, acoustic or inactive vibrational modes to the amplitude of motions. For instance, the $\langle u_{11}^2 \rangle$ term results from motions associated with acoustic modes (with a direction of propagation along $[1\bar{2}10]$ and particle displacements in the same direction) and also optical modes, including one of the lattice Raman-active modes of E_g symmetry, and one IR-active mode of E_u symmetry.

It is possible to derive the amplitude of motions associated with a given vibrational mode from lattice dynamics calculations. Such calculations are computationally intensive, and the results can depend heavily on the model force field used. An alternative approach can be adopted to obtain vibrational amplitudes directly from spectroscopic data, by considering the carbonates as molecular crystals with rigid CO_3 groups, and using the Debye-Weller model to relate frequencies and amplitudes of vibration.

We begin with the simple Debye-Waller theory of the variation with temperature of the amplitude of vibration of an atom in a monoatomic cubic crystal. In this theory, the mean square amplitude of atomic vibration $\langle u^2 \rangle$ is given by:

$$\langle u_{ii}^2 \rangle = \frac{3h^2 T}{4\pi^2 mk\theta^2}\left[\varphi(x)+\frac{x}{4}\right] \tag{2}$$

where h is Planck's constant, k is the Boltzmann constant, m is the atomic mass, $\theta=(h\nu_M/k)$, the Debye temperature and $\varphi(x)$ is defined by:

$$\varphi(x)=\frac{1}{x}\int_0^x \frac{\varepsilon d\varepsilon}{e^{\varepsilon}-1}, \tag{3}$$

with $x=\theta_M/T$ and $\varepsilon=h\nu/kT$.

Knowledge of θ_M from elastic or calorimetric measurements allows the calculation of $\langle u^2 \rangle$ as a function of T.

Cruickshank (1956) has applied and extended this formulation to the case of translational and rotational motions of rigid molecules in molecular crystals. Assuming that the dispersion of the optic modes along the Brillouin zone is small, the directionally averaged amplitude of the centre of mass (m) of a rigid molecule is given by:

$$\langle u_{ii}^2 \rangle = \frac{1}{2}\left\{\frac{3h^2 T}{4\pi^2 mk\theta^2}\left[\varphi(x)+\frac{x}{4}\right] + \frac{1}{n}\sum_1^n \frac{h}{4\pi^2 \nu_i}\coth\left(\frac{h\nu_i}{2kT}\right)\right\} \tag{4}$$

The first term of the RHS of (4) gives the contribution from the acoustic branches and the second the contribution from all the optic modes.

Similarly, the mean square amplitude of rotational vibrations is given by:

$$\langle \phi_i^2 \rangle = \left[\frac{h}{8\pi^2 In}\sum_1^n \frac{1}{\nu_i}\coth\left(\frac{h\nu_i}{2kT}\right)\right] \tag{5}$$

where I is the moment of inertia of the molecule with respect to the axis of rotation.

These simple relations have been successfully tested on several molecular crystals like anthracene (Cruickshank 1956; Brock and Dunitz 1982), terphenyl (Baudour et al. 1974), durene (Baudour and Sanquer 1974), and TlN_3 (Christoe and Iqbal 1977) to predict the evolution of vibrational amplitudes with temperature.

Equations (4) and (5) can be used in two ways. First of all, observed frequencies of optically-active vibrational modes can be used to calculate corresponding translational and librational amplitudes, and their temperature dependence. There are, however, some limitations to the method: the optic modes must be unambigously assigned to given motions (this is complicated by coupling between modes in the carbonates), and the mode frequencies must be constant across the Brillouin zone (this is not the case for carbonates: Plihal and Schaack 1970; Cowley and Pant 1973). Cruickshank (1956) has proposed a way to overcome these limitations. A vibrational amplitude measured at one temperature (usually at 300 K) by X-ray and spectroscopic measurements at various temperatures can be used to obtain vibrational amplitudes at any other temperatures. In this case the only assumption is that each L_{ii} or T_{ii} is associated with a single effective frequency, corresponding to the mean weighted frequency of all vibrational modes participating in the considered motion as expressed in (4) and (5). From (2) (or (3)), and knowing T_{ii} (or L_{ii}) at 300 K, we calculate an effective Debye temperature, or the related effective frequency ($^{eff}\nu_i$). This latter procedure has the advantage of averaging the effect of any dispersion of mode frequencies across the Brillouin zone. It is worth noting that, in either procedure, anharmonicity can be introduced via a temperature dependence of the experimental or the effective vibrational frequencies. Application of these procedures to translations and librations of the CO_3 groups in carbonates can be carried out by assuming that they behave as rigid bodies, and that (4) and (5) can be applied via consideration of only the mass and moment of inertia of CO_3. This last assumption is valid because the cations do not participate in the Raman-active lattice modes. To begin with, we use the second procedure.

Using (4) and (5) in their high-temperature limit forms, the $^{eff}\nu_i$ corresponding to the L_{ii} and T_{ii} at 300 K of calcite, dolomite and magnesite have been calculated (Table 3). For the L_{11} librations, the moment of inertia of CO_3 in the (0001) plane has been used ($I_{11}=6.63\ 10^{-46}$ kg·m^2), while for the L_{33} librations the moment of inertia perpendicular to (0001) plane has been considered ($I_{33}=1.326\ 10^{-45}$ kg·m^2). For the T_{ii}, m was taken to be $9.96\ 10^{-26}$ kg. The $^{eff}\nu_i$ for the L_{ii} lie at lower wavenumbers than those corresponding to the T_{ii}. This is consistent with the assignment of the low frequency lattice modes discussed earlier. The calculated $^{eff}\nu_i$ represent average frequencies of all the modes which motions contribute to L_{ii} and T_{ii}. Only two optic modes, one E_u (IR active) and one E_g (Raman-active), contribute to the L_{11} amplitude. The $^{eff}\nu_i$ calculated from the observed L_{11} (Table 3) are 120, 163 and 232 cm^{-1} for calcite, dolomite and magnesite, respectively. These compare favourably with the E_g Raman modes frequencies

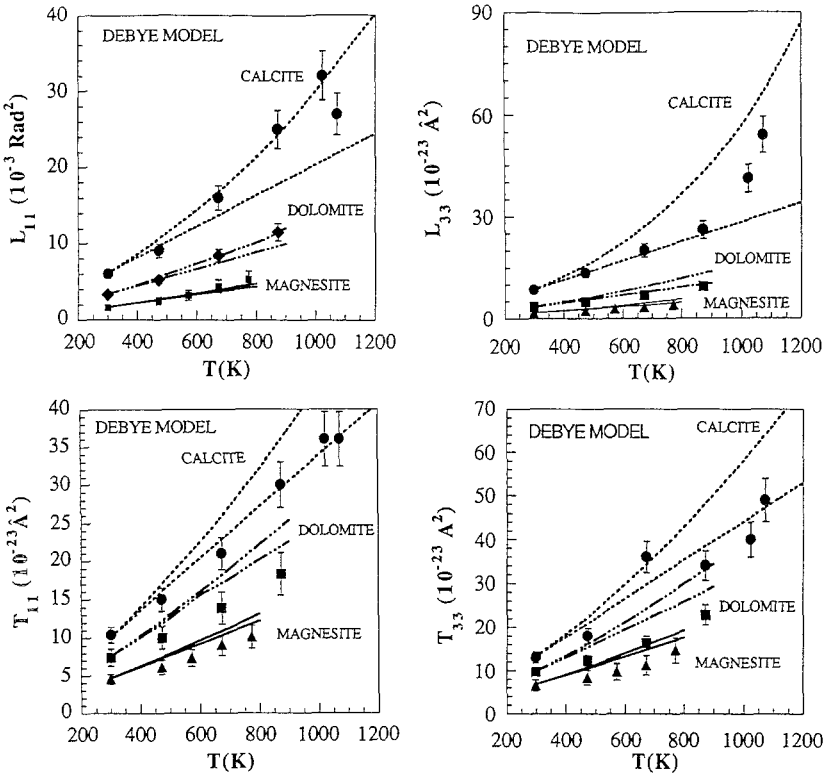

Fig. 10. TLS parameters of CO_3 in calcite, dolomite and magnesite calculated from Debye-Waller type relations given by Cruickshank (1956) ((4) and (5) in text). The room temperature frequencies, ${}^{eff}\nu_i$, for each L_{ii} and T_{ii} are given in Table 3. The linear curves are obtained by assuming that (${}^{eff}\nu_i$) is constant with temperature. The upper curves are calculated by using the measured $(\partial \nu_i/\partial T)_P$ of the Raman modes for the corresponding (${}^{eff}\nu_i$). The points represent the T_{ii} and L_{ii} data of Markgraf and Reeder (1985) and Reeder and Markgraf (1986)

Table 3. T_{ii} and L_{ii} values for calcite, magnesite and dolomite obtained by Markgraf and Reeder (1985) and Reeder and Markgraf (1986). ${}^{eff}\nu_i$ values calculated from these data using Cruikshank (1956) model (see text)

	T_{11} 10^{-23} Å^2	${}^{eff}\nu_i$ cm^{-1}	T_{33} 10^{-23} Å^2	${}^{eff}\nu_i$ cm^{-1}	L_{11} 10^{-3} Rad^2	${}^{eff}\nu_i$ cm^{-1}	L_{33} 10^{-3} Rad^2	${}^{eff}\nu_i$ cm^{-1}
Calcite	10.4	186	13.0	163	6.0	120	8.4	72
Dolomite	7.4	216	9.6	190	3.3	163	3.4	113
Magnesite	4.5	277	6.5	231	1.6	232	1.7	160

(calcite: 156, dolomite: 178 and magnesite: 213 cm^{-1}) and with the E_u IR modes (calcite: 102–123 and magnesite: 225–241 cm^{-1}) reported by White (1974). For the L_{33} amplitudes, one inactive A_{2g} and one IR-active A_{2u} mode are involved. The ${}^{eff}\nu_i$ (72, 113 and 160 cm^{-1} for calcite, dolomite and magnesite respectively) compare reasonably well with mean frequencies calculated from the A_{2u} frequencies tabulated by White (1974) for calcite (LO-TO: 92–136 cm^{-1}), dolomite (A_{2u} TO-LO: 146–193), and magnesite (LO-TO: 230–281 cm^{-1}), although, like the ${}^{eff}\nu_i$ calculated for L_{11}, they lie a little higher than the mean of the observed frequencies. This can be partly ascribed to some degree of coupling between modes at room temperature, and lack of spectroscopic information on some modes, and details of the dispersion across the Brillouin zone. Similar observations can be made for the ${}^{eff}\nu_i$ calculated from the observed T_{ii}. The T_{11} amplitude results from the combined motions of one Raman active E_g mode and one acoustic mode propagating in the [1$\bar{2}$10] direction. The ${}^{eff}\nu_i$ calculated from the observed T_{11} (Table 3) are 186, 216 and 277 cm^{-1} for calcite, dolomite and magnesite respectively. These frequencies are close to the mean average values calculated with the Raman E_g modes (calcite: 281 cm^{-1}; dolomite: 300 cm^{-1}; magnesite: 329 cm^{-1}) and acoustic modes along [1$\bar{2}$10] (calcite: 133 cm^{-1}, dolomite: 155 cm^{-1}; magnesite: 176 cm^{-1}). Similarly, the L_{33} amplitudes result from the combined motions of one IR-active E_u mode and one acoustic mode propagating in the [0001] direction.

The T_{ii} and L_{ii} amplitudes have then been calculated as a function of temperature using relations (4) and (5), either assuming a constant ${}^{eff}\nu_i$, or by introducing a temperature dependence of ${}^{eff}\nu_i$. It was assumed that the $(\partial \nu_i/\partial T)_P$ of the Raman modes (Table 2) are representative of those of the ${}^{eff}\nu_i$. The results (Fig. 10) show that this simple theory gives calculated displacement amplitudes in excellent agreement with, the X-ray data. Moreover, a better agreement is observed when a temperature-dependence for the frequencies is allowed. The strong non-linear behaviour of the L_{ii} displacements with temperature, observed in the X-ray structure refinements for calcite, is only reproduced in these calculations if the temperature dependence of the frequencies is taken into account. The better agreement between calculated and observed values for some amplitudes compared to

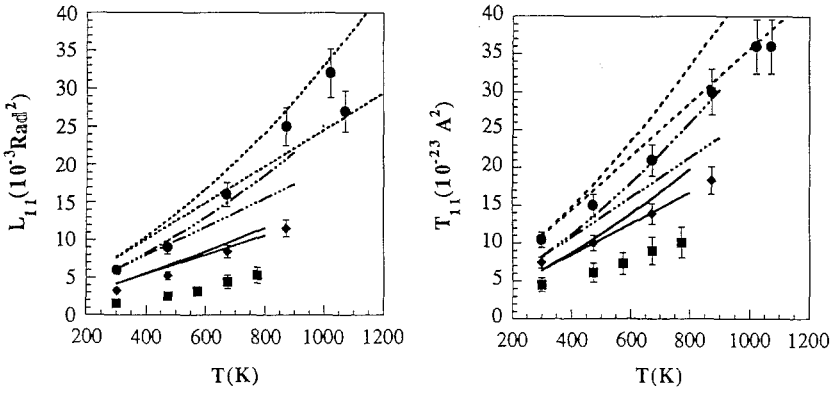

Fig. 11. T_{11} and L_{11} amplitudes of CO_3 in calcite, dolomite and magnesite. The curves are calculated directly from experimental Raman and acoustic data (see text for details)

Table 4. Isothermal and isobaric Grüneisen and mode anharmonic parameters of calcite, aragonite and dolomite

Aragonite				Dolomite				Calcite				Magnesite			
ν_i cm^{-1}	γ_{iT} [a]	γ_{iP} [b]	a_i $(10^{-5}\,K^{-1})$	ν_i cm^{-1}	γ_{iT} [c]	γ_{iP} [d]	a_i $(10^{-5}\,K^{-1})$	ν_i cm^{-1}	γ_{iT} [e]	γ_{iP} [f]	a_i $(10^{-5}\,K^{-1})$	ν_i cm^{-1}	γ_{iT} [g]	γ_{iP} [h]	a_i $(10^{-5}\,K^{-1})$
155	1.2	2.7	−7.2												
180	2.6	2.1	+3.4	178	0.9	4.4	−8.4	156	1.2	19.9	−16.9	213	2.6	2.4	0.3
209	1.2	3.0	−11.6												
				300	1.4	4.4	−7.3	281	1.4	15.8	−13.0	329	1.7	3.0	−2.5
				335	0.8	2.3	−3.7								
702	0.14	0.0	+0.9	724	0.2	0.12	+0.2	711	0.23	0.62	−0.3	738	0.23	0.00	0.44
710	0.20	0.3	−0.9												
1084	0.16	0.21	−0.2	1097	0.25	0.24	0.0	1085	0.40	0.51	−0.1	1094	0.28	0.17	0.21
				1439	0.23	1.01	−1.9	1434	0.46	1.94	−1.3	1444	0.34	1.08	−1.42
				1750	−0.02	0.03	−0.1	1748	−0.04	0.34	−0.34	1762	−0.03	0.76	−1.52

[a] Calculated with $K_T = 64.5$ GPa (Martens et al. 1982)
[b] Calculated with $\alpha_0 = 6.5\ 10^{-5}\ K^{-1}$ (Salje and Viswanathan 1976)
[c] Calculated with $K_T = 94$ GPa (Ross and Reeder 1992)
[d] Calculated with $\alpha_0 = 2.41\ 10^{-5}\ K^{-1}$ (Reeder and Markgraf 1986)
[e] Calculated with $K_T = 73$ GPa (Martens et al. 1982). [f] Calculated with $\alpha_0 = 0.9\ 10^{-5}\ K^{-1}$ (Markgraf and Reeder 1985). [g] Calculated with $K_T = 122$ GPa (Martens et al. 1982). [h] Calculated with $\alpha_0 = 1.93\ 10^{-5}\ K^{-1}$ (Markgraf and Reeder 1985)

others is most likely due to the quasi-harmonic assumptions underlying the calculations, or to the occurrence of mode mixing.

Calculations were also carried using the first procedure described above, i.e., calculations of the T_{ii} and L_{ii} from the actual IR and Raman data at k = 0, and acoustic frequencies. However, as emphasized previously, all the modes involved in a given amplitude of motion are not known experimentally, and their dispersion across the Brillouin zone is only poorly constrained. As a consequence the agreement with observed values is only fair. For example, calculated L_{11} and T_{11} amplitudes from (4) and (5) are shown in Fig. 11. For the T_{11} displacement, one Raman active E_g mode (at 281 cm^{-1} in calcite, 329 cm^{-1} in magnesite and 300 cm^{-1} in dolomite) and one acoustic mode propagating in the [1$\bar{2}$10] direction has been considered. For L_{11}, one E_g mode (155 cm^{-1} in calcite, 213 cm^{-1} in magnesite and 178 cm^{-1} in dolomite) has been used in the calculations. The calculated values (curves in Fig. 11) reproduce only qualitatively the X-ray data. However they do account for the relative behaviour of the three minerals and for the temperature dependence of the amplitudes.

Mode Grüneisen und Anharmonic Parameters

The effects of pressure or temperature on vibrational mode frequencies can be expressed by $(\partial \ln \nu_i/\partial P)_T$ or $(\partial \ln \nu_i/\partial T)_P$, or by $(\gamma_{iT} = K_T(\partial \ln \nu_i/\partial P)_T$, the classical mode Grüneisen parameter and its isobaric equivalent $\gamma_{iP} = (-1/\alpha)(\partial \ln \nu_i/\partial T)_P)$ (Gillet et al. 1989). From these mode parameters one can define an anharmonic parameter a_i for each observed mode (Gillet et al. 1989):

$$a_i = \alpha(\gamma_{iT} - \gamma_{iP})$$

Values of these parameters are given in Table 4. They have been calculated with the initial slopes of the $\nu(T)$ and $\nu(P)$ curves. For the four carbonates studied, the absolute values of these a_i parameters are small (close to 0) for the internal modes of the CO_3 groups, and large for the lattice modes. Such a difference between internal and lattice modes has already been observed in other minerals (Gillet et al. 1989, 1990, 1991, 1992; Fiquet et al. 1992). The overall anharmonic behaviour of carbonates is thus due to the lattice modes, i.e., to vibrational degrees of freedom involving the Mg−O and Ca−O bonds, rather than to the internal vibrations of

the CO_3 groups, consistent with the discussion throughout this paper. The a_i parameters of the librational and translational modes are higher in calcite than in magnesite, dolomite having intermediate values, indicating a more pronounced anharmonicity in calcite, also consistent with the other data discussed in this paper. As already discussed (Gillet et al. 1990; Gillet et al. 1991) the a_i parameters are temperature-dependent. This temperature dependence will be discussed in a companion paper (Gillet et al. in prep.) along with the calculation of the heat capacities and vibrational entropies of calcite, dolomite and magnesite, and $^{18}O/^{16}O$ isotopic fractionation factors, via the models developed by Kieffer (1979).

Acknowledgements. This work was financially supported by the French programme DBT (Minéraux, Fluides et Cinétiques). INSU contribution n° 530. A Lakhrissi is thanked for his help in the high-temperature Raman experiments. P.F. McMillan was partly supported by an NSF-CNRS travel grant; he also thanks the Université de Rennes I for a visiting professorship during this work.

References

Baudour JL, Sanquer M (1974) A constrained refinement of the structure of durene including "wagging" vibrations of the methyl groups. Acta Crystallogr B30:2371–2378

Baudour JL, Delugeard Y, Sanquer M (1974) On the isomorphism of p-terphenyl and phenyl isocyanate dimer. Acta Crystallogr B30:691–696

Biellmann C, Gillet Ph (1992) High-pressure and high-temperature behaviour of calcite, aragonite and dolomite: a Raman spectroscopic study. Eur J Mineral 4:389–393

Biellmann C, Gillet Ph, Guyot F, Peyronneau J, Raynard B (1992) Experimental evidence for carbonates stability in the Earth's lower mantle. Earth Planet Sci Lett (submitted)

Birch F (1966) Compressibility: Elastic constants. In: Clark SP, Jr (ed) Handbook of Physical Constants. Geol Soc Am Mem 97, Geol Soc Am, Boulder, CO, pp 107–173

Bischoff WD, Sharma SK, Mackenzie FT (1985) Carbonate ion disorder in synthetic and biogenic magnesian calcites: a Raman spectral study. Am Mineral 70:581–589

Bréhat F, Wyncke B (1985) Analysis of the temperature-dependent infrared active lattice modes in the ordered phase of sodium nitrate. J Phys C 18:4247–4259

Bridgman PW (1939) The high-pressure behaviour of miscellaneous minerals. Am J Sci 37:7–18

Brock CP, Dunitz JD (1982) Temperature dependence of thermal motion in crystalline naphthalene. Acta Crystallogr B38:2218–2228

Cabannes J (1942) Symétrie des oscillations fondamentales. Rev Sci 80:407

Christoe CW, Iqbal Z (1977) Raman scattering study of the dynamics of the pressure-induced phase transition in thallium azide (TlN_3). J Phys Chem Solids 38:1391–1394

Collerson B, Williams Q, Knittle E (1991) Vibrational spectra of $MgCO_3$-magnesite and $CaCO_3$ (III) at high pressures. EOS Trans Am Geophys Union 72:436

Couture L (1947) Etude des spectres de vibrations de monocristaux ioniques. Ann Phys. 12:5–65

Cowley ER, Pant AK (1973) Lattice dynamics of calcite. Phys Rev B 8:4795–4800

Cruikshank DWJ (1956) The variation of vibration amplitudes with temperature in some molecular crystals. Acta Crystallogr 9:1005–1009

Dove MT, Powell BM (1989) Neutron diffraction study of the tricritical orientational order/disorder phase transition in calcite at 1260 K. Phys. Chem Minerals 16:503–507

Farmer VC (1974) The infrared spectra of minerals. Mineralogical Society, London

Fiquet G, Gillet Ph, Richet P (1992) Anharmonicity and high-temperature heat capacity of crystals: the examples of Mg_2GeO_4, Ca_2GeO_4, $MgCaGeO_4$ olivines. Phys Chem Minerals 18:469–479

Fong MY, Nicol M (1971) Raman spectrum of calcium carbonate at high-pressures. J Chem Phys. 54:579–585

Frech R, Wang EC, Bates JB (1980) The IR and Raman spectra of $CaCO_3$ (aragonite). Spectrochim Acta 36A:915–919

Gillet Ph, Gérard Y, Willaime C (1987) The calcite-aragonite transition: mechanism and microstructures induced by the transformation stresses and strain. Bull Minéral 110:481–496

Gillet Ph, Malezieux JM, Dhamelincourt MC (1988) Microraman multichannel spectroscopy up to 2.5 GPa using a sapphire-anvil cell: experimental set-up and some applications. Bull Minéral 111:1–15

Gillet Ph, Guyot F, Malézieux JM (1989) High pressure and high temperature Raman spectroscopy of Ca_2GeO_4: some insights on anharmonicity. Phys Earth Planet Inter 58:141–154

Gillet Ph, Le Cléac'h A, Madon M (1990) High-temperature Raman spectroscopy of the SiO_2 and GeO_2 polymorphs: anharmonicity and thermodynamic properties at high-temperature. J Geophys Res B95:21635–21655

Gillet Ph, Richet P, Guyot F, Fiquet G (1991) High-temperature properties of forsterite. J Geophys Res, B96:11805–11816

Gillet Ph, Fiquet G, Malézieux JM, Geiger C (1992) High-pressure and high-temperature Raman spectroscopy of end-member garnets: pyrope, grossular and andradite. Eur J Mineral 4:651–664

Griffith WP (1969) Raman spectroscopy of minerals. Nature 224:264–266

Hellwege KH, Lesch W, Plihal M, Schaack G (1970) Zwei-Phononen-Absorptionsspektren und Dispersion der Schwingungszweige in Kristallen der Kalkspatstruktur. Z. Phys. 232:61–86

Herzberg G (1945) Molecular spectra and molecular structure. II. Infrared and Raman spectra of polyatomic molecules. Van Nostrand, New York

Hexter RM (1958) High-resolution, temperature-dependent spectra of calcite. Spectros Chim Acta 10:281–290

Irving AJ, Wyllie PJ (1975) Subsolidus and melting relationships for calcite, magnesite and the joint $CaCO_3-MgCO_3$ to 36 kb. Geochim Cosmochim Acta 39:35–53

Jacobson JL, Nixon ER (1968) Infrared dielectric response and lattice vibrations of calcium and strontium oxydes. J Phys Chem Solids 29:967–976

Katsura T, Ito E (1990) Melting and subsolidus phase relations in the $MgSiO_3-MgCO_3$ system at high-pressures: implications to evolution of the Earth's atmosphere. Earth Planet Sci Lett 99:110–117

Kieffer SW (1979) Thermodynamics and lattice vibrations of minerals: 3. Lattice dynamics and an approximation for minerals with application to simple substances and framework silicates. Rev Geophys Space Phys 17:827–849

Kraft S, Knittle E, Williams Q (1991) Carbonate stability in the Earth's mantle: a vibrational study of aragonite and dolomite at high pressures and temperatures. J Geophys Res 96:17997–18009

Krishnamurti D (1956) Raman spectrum of magnesite. Proc Indian Ac Sci A43:210–212

Krishnamurti D (1957) The Raman spectrum of calcite and its interpretation. Proc Indian Ac Sci A46:183–202

Liu LG, Mernagh TP (1990) Phase transitions and Raman spectra of calcite at high pressures and room temperature. Am Mineral 41:745–756

Markgraf SA, Reeder RJ (1985) High temperature structure refinements of calcite and magnesite. Am Mineral 70:590–600

Martens R, Rosenhauer M, Gehlen Kv (1982) Compressibilities of carbonates. In: W Schreyer (ed) High Pressure Researches in Geoscience. Schweizerbart'sche, Stuttgart, pp 215–222

Megaw HD (1970) Thermal vibrations and a lattice mode in calcite and sodium nitrate. Acta Crystallogr A26:236–244

Merrill L, Bassett WA (1975) The crystal structure of $CaCO_3$ (II), a high-pressure meteastable phase of calcium carbonate. Acta Crystallogr B31:343–349

Neuman G, Vogt H (1978) Rayleigh wing scattering in disordered sodium nitrate. Phys Status Solidi 85:179–184

Nicola JH, Scott JF, Couto RM, Correra MM (1976) Raman spectra of dolomite ($CaMg(CO_3)_2$). Phys. Rev B14:4676–4678

Piriou B (1974) Etude des modes normaux par réflexion infrarouge. Ann Chim 9:9–17

Plihal M, Shaack G (1970) Lattice dynamics of calcite structure. I. Normal frequencies and normal modes at zero wave vectors. Phys Status Solidi 42:495–506

Plihal M (1973) Lattice dynamics of calcite structure. II. Dispersion curves and phonons densities. Phys Status Solidi 56:485–496

Porto SPS, Giordmaine JA, Damen TC (1966) Depolarization of Raman scattering in calcite. Phys Rev 147:608–611

Redfern SAT, Salje E, Navrotsky A (1989) High-temperature enthalpy at the orientational order-disorder transition in calcite: implications for the calcite/aragonite phase equilibrium. Contrib Mineral Petrol 101:479–484

Reeder RJ (ed) (1983) Carbonates: Mineralogy and Chemistry. Rev Mineral 11. Mineralogical Society Washington DC, pp 394

Reeder RJ, Markgraf SA (1986) High-temperature crystal chemistry of dolomite. Am Mineral 71:769–776

Ross SD (1972) Inorganic Infrared and Raman spectroscopy. McGraw-Hill, New York

Ross NL, Reeder RJ (1992) High pressure structural study of dolomite and ankerite. Am Mineral 77:412–421

Rousseau DL, Miller RE, Leroi GE (1968) Raman spectrum of crystalline sodium nitrate. J Chem Phys 48:3409–3413

Rutt HN, Nicola JH (1974) Raman spectra of carbonates of calcite structure. J Phys C 7:4522–4528

Salje E, Viswanathan K (1976) The phase diagram calcite-aragonite as derived from the crystallographic properties. Contrib Mineral Petrol 55:55–77

Sakurai T, Sato T (1971) Temperature dependence of vibrational spectra in calcite by means of emissivity measurement. Phys. Rev B4:583–591

Schmahl WW, Salje E (1989) X-Ray diffraction study of the orientational order/disorder transition in $NaNO_3$: evidence for order parameter coupling. Phys Chem Minerals 16:790–798

Schroeder RA, Weir CE, Lippincott ER (1962) Lattice frequencies and rotational barriers for inorganic carbonates and nitrates from low-temperature infrared spectroscopy. J Res Natn Bur Stand 66A:407–434

Shen TY, Mitra SS, Prask H, Trevino SF (1975) Order-disorder phenomenon in sodium nitrate studied by low frequency Raman scattering. Phys Rev B12:4530–4533

Vo-Than, Lacam A (1984) Experimental study of the elasticity of single crystalline calcite under high pressure (the calcite I-calcite II transition at 14.6 kbar). Phys Earth Planet Inter 34:195–203

White WB (1974) The carbonate minerals. In: Farmer VC (ed) The Infrared spectra of minerals, Mineralogical Society, London, pp 87–110

Yasaka H, Sakai A, Yagi T (1985) A central peak in the order-disorder phase transition of sodium nitrate. J Phys Soc Japan 54:3697–3700